Food Chemistry: X 25 (2025) 102127

Contents lists available at ScienceDirect

Food Chemistry: X

journal homepage: www.sciencedirect.com/journal/food-chemistry-x

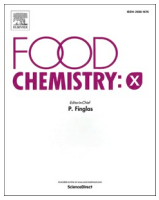

Quality analysis of *Idesia polycarpa* fruit oil samples from cultivars with different phenotypes

Tianting Luo [a,1], Jiaqi Xu [a,1], Zhouqin Zhen [a], Xue Pan [a], Lang Feng [b], Likang Qin [a], Tingyuan Ren [a,*]

[a] College of Brewing and Food Engineering, Guizhou University, Guiyang 550025, Guizhou, China
[b] School of Mechanical Engineering, Guizhou University, Guiyang 550025, Guizhou, China

ARTICLE INFO

Keywords:
Idesia polycarpa fruit oil (*IPFO*)
Traits
Aroma composition
Fatty acid composition

ABSTRACT

To study the quality characteristics of *Idesia polycarpa* fruit oil (*IPFO*) samples under varying phenotypic traits and their differences, three typical phenotypic fruits of the same cultivar were compared, both morphologically and chemically. The results revealed that the highest water content (51.90 %) occurred in small red fruits (RID-S), and the highest oil content (20.63 %) was obtained in large yellow fruits (YID). A total of 532 aroma compounds were identified via gas chromatography–mass spectrometry (GC–MS), with terpenes as the major contributors. The fatty acid composition was dominated by linoleic acid (LA), palmitic acid and oleic acid, and the LA content was highest in large red fruits (RID-B) (1633.25–1807.21 μg/mL), whereas the palmitic acid and oleic acid contents were highest in YID (863.72–976.70 μg/mL and 505.96–604.04 μg/mL, respectively). The oil quality of *I. polycarpa* varied according to its phenotypic characteristics, with RID-B identified as an excellent cultivar, followed by YID and RID-S.

1. Introduction

Idesia polycarpa belongs to the *Flacourtiaceae* family and is a high-quality, high-yielding woody oilseed crop. It is found mainly in southwestern China (Shang et al., 2024). Many wild *I. polycarpa* plants are distributed in Guizhou, which is a suitable and favorable area. The fruit of *I. polycarpa* has a high oil content, with an oil yield approximately 6.7 times greater than that of soybean and 4 times greater than that of rape, resulting in the name of the tree oil bank(Zuo et al., 2024). China is the first country in which edible oil is consumed. According to the National Cereals and Oils Information Centre data, from 2021 to 2022, China's vegetable oil imports were 12.65 million tons, of which 6.82 million tons of palm oil, 2.51 million tons of vegetable oil, 1.64 million tons of rapeseed oil, 1.23 million tons of soybean oil and 120,000 tons of peanut oil once again hit a record high. High imports of vegetable oils have led to rising domestic prices. The development of new vegetable oils positively affects market pressure and economic development conditions. China encompasses rich resources of oil plants, of which there are more than 400 species of woody oil trees, but only a dozen of these species are being developed and used at present. The development of *I. polycarpa* fruit oil (*IPFO*) not only enriches the species that provides edible woody oil but also solves the problem in which the domestic production capacity is insufficient. Moreover, *IPFO* is an important industrial raw material resource that is usually used in the manufacture of paints, lubricants, soaps, and biodiesel(Dyer et al., 2008; Lummiss et al., 2012). Therefore, *IPFO* provides new ways to resolve the shortages of edible oil, industrial oil, energy and other raw materials(Wen et al., 2022).

The content and composition of fruit oils constitute one of the main study areas for *I. polycarpa* because *IPFO* is high in polyunsaturated fatty acids, especially linoleic acid (LA), which has a relatively low content in most vegetable oils (e.g., olive oil and tea oil)(Mena et al., 2018; Shi et al., 2020). LA is an essential human dietary fatty acid that cannot be synthesized in the body and must be obtained from external sources to meet health needs. Research has indicated that LA is an important factor in fetal and infant development(Bowen & Clandinin, 2005), as well as in the pathogenesis of hypertension(Eguchi et al., 2012) and diabetes (Marangoni et al., 2020). Furthermore, *IPFO* has been employed in the development of conjugated linoleic acid (CLA). However, previous studies have indicated that there are significant variations in the morphology, chemical composition and flavor of *I. polycarpa* from

* Corresponding author.
E-mail address: tyren@gzu.edu.cn (T. Ren).
[1] Contributed equally to this work.

https://doi.org/10.1016/j.fochx.2024.102127
Received 2 November 2024; Received in revised form 14 December 2024; Accepted 20 December 2024
Available online 24 December 2024
2590-1575/© 2024 The Author(s). Published by Elsevier Ltd. This is an open access article under the CC BY-NC-ND license (http://creativecommons.org/licenses/by-nc-nd/4.0/).

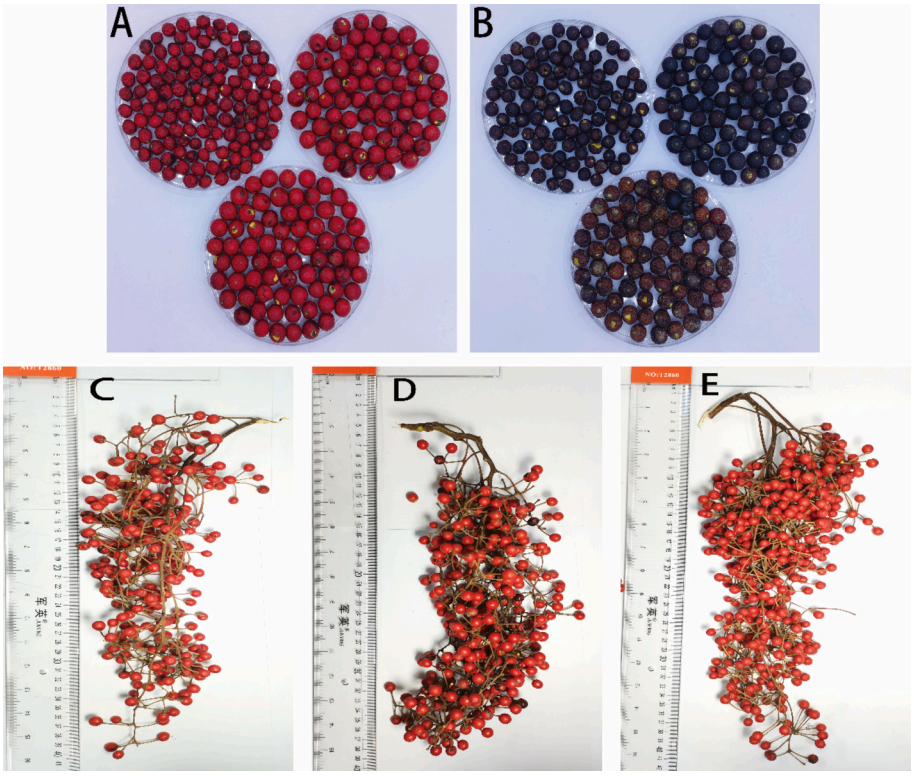

Fig. 1. Fresh (A) and dry (B) samples of *I. polycarpa* fruits exhibiting diverse phenotypic traits and morphological variations: RID-S (C), RID-B (D), and YID (E).

Table 1
Fruit phenotypic traits of *Idesia polycarpa*.

Statistic	Variety		
	RID-S	RID-B	YID
SL/mm	34.20 ± 1.53^{ab}	36.93 ± 1.27^{a}	32.40 ± 1.35^{b}
SW/mm	14.80 ± 1.05^{b}	14.13 ± 0.38^{b}	16.43 ± 0.81^{a}
SAR/mm	2.32 ± 0.08^{b}	2.61 ± 0.05^{a}	1.97 ± 0.02^{c}
NFPS/pcs	418 ± 130^{a}	318 ± 9^{a}	354 ± 80^{a}
PMSS/g	14.91 ± 1.13^{a}	16.56 ± 1.81^{a}	16.31 ± 1.23^{a}
FMSS/g	71.06 ± 10.79^{a}	75.40 ± 3.03^{a}	76.92 ± 8.50^{a}
SSM/g	89.22 ± 10.72^{a}	94.85 ± 4.53^{a}	95.24 ± 9.72^{a}
FTD/mm	8.12 ± 0.23^{b}	10.46 ± 0.29^{a}	8.36 ± 0.51^{b}
FLD/mm	7.92 ± 0.65^{b}	10.28 ± 0.19^{a}	8.38 ± 0.29^{b}
FShI/mm	0.98 ± 0.06^{a}	0.98 ± 0.01^{a}	1.00 ± 0.03^{a}
FSiI/mm	64.35 ± 6.12^{b}	107.55 ± 4.31^{a}	70.16 ± 6.59^{b}
SFM/g	0.21 ± 0.04^{b}	0.56 ± 0.04^{a}	0.26 ± 0.04^{b}
FSL/mm	14.07 ± 2.60^{a}	17.17 ± 1.85^{a}	13.67 ± 1.59^{a}

Note: Spike length (SL), spike width (SW), spike aspect ratio (SAR), number of fruit per spike (NFPS), petiole mass of single spike (PMSS), fruit mass of single spike (FMSS), single spike mass (SSM), fruit transverse diameter (FTD), fruit longitudinal diameter (FLD), fruit shape index (FShI), fruit size index (FSiI), single fruit mass (SFM), and fruit stalk length (FSL). Fruit shape index (FShI): Fruit longitudinal diameter (FLD)/Fruit transverse diameter (FTD). Fruit size index (FSiI): Fruit longitudinal diameter (FLD) * Fruit transverse diameter (FTD). "a, b" indicates a significant difference ($P < 0.05$).

different regions in China. These differences directly impact the efficiency and economic value of *IPFO* in various applications. Notably, the study of fruit oils from *I. polycarpa* with differing phenotypic traits within a single variety has yet to be reported. Thus, by studying the color, fruit oil flavor and oil composition of *IPFOs* of the same variety with different phenotypic characteristics, *I. polycarpa*, which has a high yield, good color, high oil yield and good quality, was selected, cultivated and promoted.

To examine the nutritional and flavor-associated metabolites of fruit oils from *I. polycarpa* with varying phenotypic characteristics, headspace solid–phase microextraction (HS-SPME) was employed in conjunction with gas chromatography–mass spectrometry (GC–MS) and an electronic nose to comprehensively analyze the differences in the respective characteristic metabolites and fat composition of fruit oils from an identical cultivar of *I. polycarpa* with different typical phenotypic attributes. The combination of color and phenotypic characteristics in this study contributes to the selection and breeding of superior *I. polycarpa* varieties and facilitates the advancement of functional food products. This study provides a systematic basis for the development and application of *IPFO*, promoting its sustainable development in terms of health, environmental protection and the economy.

2. Materials and methods

2.1. Materials and reagents

Petroleum ether was purchased from Tianjin Fuyu Fine Chemical Co. (Tianjing, China). Hexane (chromatographic purity) was purchased from Shanghai Amperexperiment Technology Co. (Shanghai, China). Methyl tert-butyl ether (chromatographic purity) and formic acid (chromatographic purity) were purchased from Merck Pharmaceutical Biotechnology (Beijing, China). Sodium chloride (pure analysis) was purchased from Sinopharm Chemical Reagent Co. (Shanghai, China). Phosphoric acid (chromatographically pure) was purchased from Nanjing Chemical Reagent Co. (Nanjing, China). A 15 % methanol solution of boron trifluoride (chromatographically pure) was purchased from Shanghai Eon Chemical Technology Co. (Shanghai, China).

2.2. Sample preparation

Mature hairy-leafed *I. polycarpa* samples were harvested from six experimental bases, each of which was selected and tested by Guizhou Xulin Agricultural Science and Technology Limited Liability Company. A total of 20 plants were obtained from each base. Samples with identical characteristics from the six bases were mixed into one

Table 2
Correlation analysis of *Idesia polycarpa* fruit traits.

Trait	SL	SW	SAR	NFPS	PMSS	FMSS	SSM	FTD	FLD	FShI	FSiI	SFM	FSL	FMC
SW	−0.478													
SAR	0.842**	−0.874**												
NFPS	0.03	0.403	−0.257											
PMSS	0.065	0.042	0.033	0.065										
FMSS	0.177	0.533	−0.237	0.602	0.486									
SSM	0.187	0.438	−0.172	0.572	0.602	0.986**								
FTD	0.624	−0.597	0.712*	−0.38	0.413	0.158	0.247							
FLD	0.635	−0.487	0.654	−0.354	0.451	0.168	0.246	0.942**						
FShI	0.027	0.333	−0.18	0.068	0.163	0.045	0.019	−0.148	0.191					
FSiI	0.648	−0.555	0.702*	−0.377	0.441	0.161	0.246	0.986**	0.984**	0.017				
SFM	0.705*	−0.479	0.687*	−0.32	0.457	0.271	0.345	0.960**	0.957**	0.014	0.976**			
FSL	0.578	−0.475	0.618	−0.639	−0.29	−0.286	−0.307	0.503	0.48	−0.088	0.509	0.574		
FMC	0.811**	−0.588	0.813**	−0.372	0.278	0.117	0.173	0.926**	0.928**	0.011	0.945**	0.967**	0.707*	
FOC	−0.573	0.32	−0.494	0.044	−0.192	−0.020	−0.063	−0.535	−0.663	−0.421	−0.614	−0.581	−0.245	−0.571

Note: Spike length (SL), spike width (SW), spike aspect ratio (SAR), number of fruit per spike (NFPS), petiole mass of single spike (PMSS), fruit mass of single spike (FMSS), single spike mass (SSM), fruit transverse diameter (FTD), fruit longitudinal diameter (FLD), fruit shape index (FShI), fruit size index (FSiI), single fruit mass (SFM), and fruit stalk length (FSL). Fruit moisture content: FMC; fruit oil content: FOC. "*" indicates a significant correlation at the 0.05 level; "**" indicates a highly significant correlation at the 0.01 level.

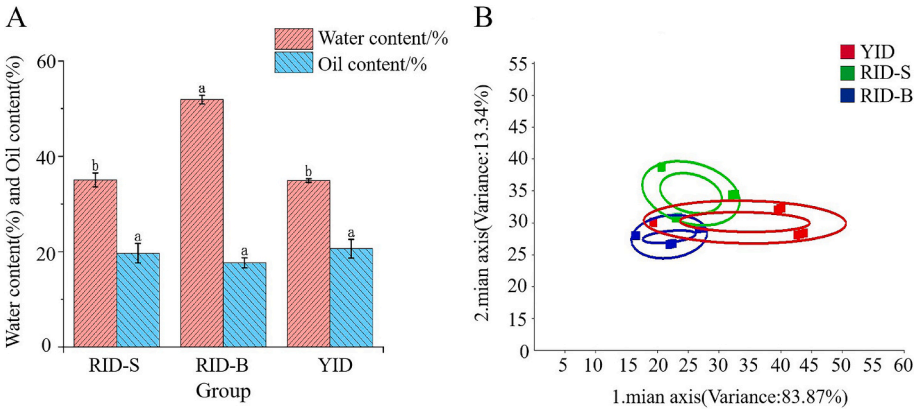

Fig. 2. Physicochemical characterization of *IPFO*. (A) Fruit water and oil contents. (B) *E*-nose PCA plot of *IPFO*. The horizontal coordinate S scale 1 main axis indicates the first principal component score value (83.87 %), the vertical coordinate 2 main axis indicates the second principal component score value (13.34 %), and the circle indicates the 95 % confidence interval.

representative sample in east–west, north–south, and central patterns, and 2 kg of each sample was then obtained, which was dried via hot air and placed aside.

2.3. Color determination

The fruit skin color of fresh and dried samples of *I. polycarpa* (Wu et al., 2023) was measured via a colorimeter (SC-10, 3nh, Shenzhen, China). Color data were recorded at each measurement point, including parameters such as brightness (L* value), redness-greenness (a* value) and yellowness-blueness (b* value), and the average of three measurements was calculated and analyzed.

2.4. Fruit phenotypic trait determination

The phenotypic traits of the sample fruits were determined according to a previously published method (Zhao et al., 2024). A total of 10 ears were selected from each plant as different-phenotypic fruit samples, and the ears were suspended vertically. The ear length (the straight line distance from the base to the top of the ear) and ear width (the maximum diameter of the ear cross section) were measured via a ruler (with an accuracy of 0.1 mm). Vernier calipers (with an accuracy of 0.1 mm) were used to measure the fruit transverse diameter, fruit longitudinal diameter and fruit stalk length. The single-fruit mass, petiole mass of a single spike, fruit mass of a single spike and single-spike mass were measured via an electronic balance (with an accuracy of 0.001 g). The number of fruits on each spike was manually counted. Concurrently, the spike aspect ratio (spike length/spike width), fruit shape index (fruit longitudinal diameter/fruit transverse diameter) and fruit size index (fruit longitudinal diameter*fruit transverse diameter) were calculated.

2.5. Determination of the fruit moisture and oil contents

The moisture content was determined according to GB 5009.3-2016 (Determination of Moisture in Food). The moisture content can be calculated as follows:

$$A\Big/\% = \frac{W_1 - W_2}{W_1 - W_3} \times 100$$

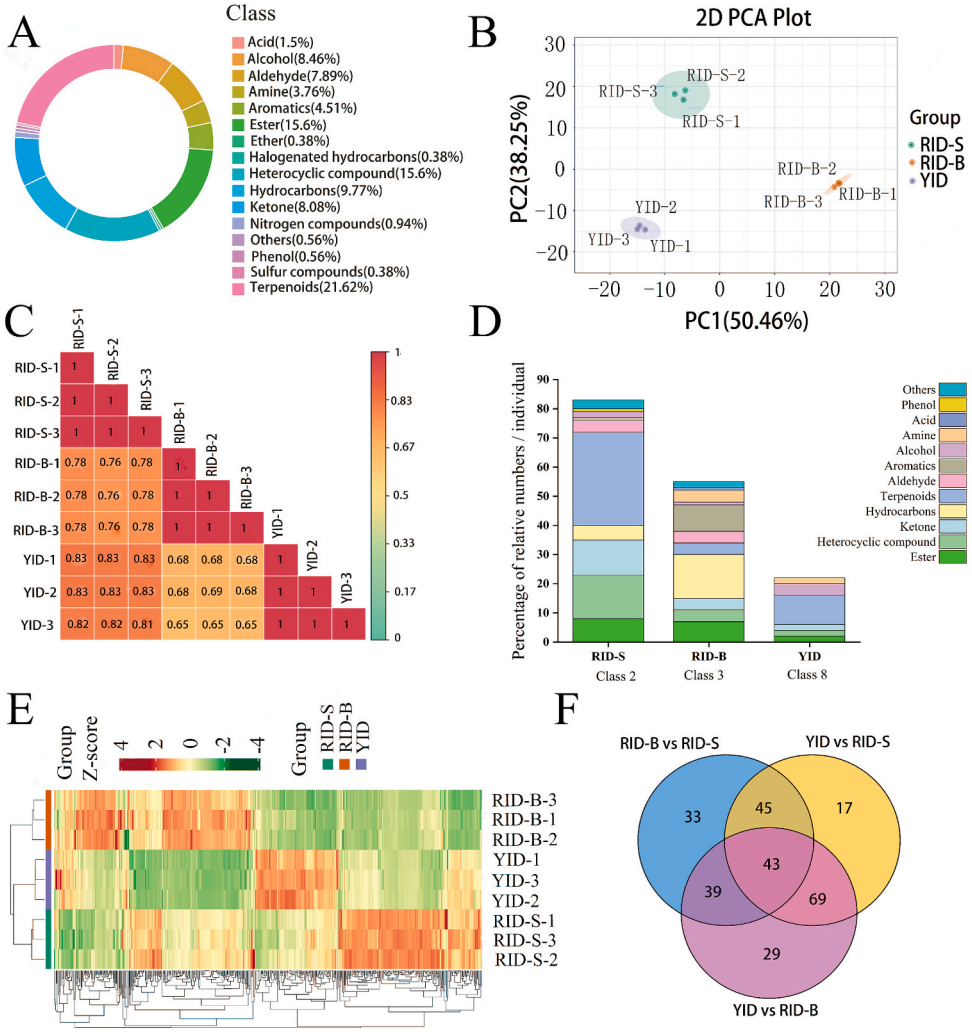

Fig. 3. Analysis of volatile metabolites associated with three distinct phenotypic traits of *I. polycarpa*. (A) Circular plot of the identified metabolite class compositions. (B) The overall metabolite PCA plots illustrate the first principal component score value (horizontal coordinate PC1) and the second principal component score value (vertical coordinate PC2) for each metabolite. The circles indicate 95 % confidence intervals. (C) Correlation plot. The use of different colors represents the strength of the Pearson correlation coefficient. Redder colors indicate a stronger positive correlation, greener colors indicate a weaker correlation, and bluer colors indicate a stronger negative correlation. (D) Composition, type, and quantity of distinctive metabolites in various *I. polycarpa* fruits. (E) Clustering heatmap. The different colors represent the values obtained from the standardization treatment of the relative contents (red represents high content and green represents low content). (F) Venn diagram of differentially abundant metabolites. Each circle in the plot represents a comparison group, and the numbers in the overlapping part of the circles represent the number of differentially abundant metabolites shared between the comparison groups. The numbers without overlapping parts represent the number of differentially abundant metabolites specific to the comparison groups. (For interpretation of the references to color in this figure legend, the reader is referred to the web version of this article.)

where A denotes the moisture content (%), W_1 denotes the mass of the lead box and the sample (g), W_2 denotes the mass of the lead box and the sample after drying (g), and W_3 denotes the mass of the lead box (g).

The Soxhlet extraction method (Liu et al., 2023) was adopted. The dried fruits of *I. polycarpa* were ground into a powder, 3–5 g of each sample was weighed into a filter tube, petroleum ether was added to 2/3 of the receiving bottle volume, various parts of the extractor were connected, and the receiving bottle was heated in a water bath at 40 °C for 8 h. After heating, the bottle was removed, and the remaining petroleum ether was collected. When 1–2 mL of petroleum ether remained in the receiving bottle, it was evaporated in a water bath, and the bottle was then dried at 105 °C for 2 h, cooled in a dryer for 0.5 h and weighed. The crude oil of *I. polycarpa* was subsequently collected. The oil content can be calculated as follows:

$$X = \frac{(m_1 - m_0)}{m_2} \times 100\%$$

where x is the oil extraction rate (%), m_1 is the mass of the receiving bottle and oil after drying to a constant weight (g), m_0 is the mass of the receiving bottle (g), and m_2 is the mass of the sample (g).

2.6. Refining of essential oils

Oil refining includes degumming, neutralization, bleaching and deodorization steps. The methods of Chakraborty and Joseph (2015) were used with modifications(Šimat et al., 2019). First, the extracted crude oil was added to a certain amount of phosphoric acid at 70 °C, cooled to room temperature and then centrifuged at 10,000 r/min for 10 min to remove precipitated gums (degumming). Next, a certain amount of sodium hydroxide solution was added dropwise to the degummed oil, heated under stirring at 60 °C for 20 min for complete neutralization, heated at 70 °C for 20 min after the pH reached 7.0, cooled and centrifuged (10,000 r/min, 10 min). The collected oil was heated under vacuum with stirring (500 rpm, 50 °C), washed three times

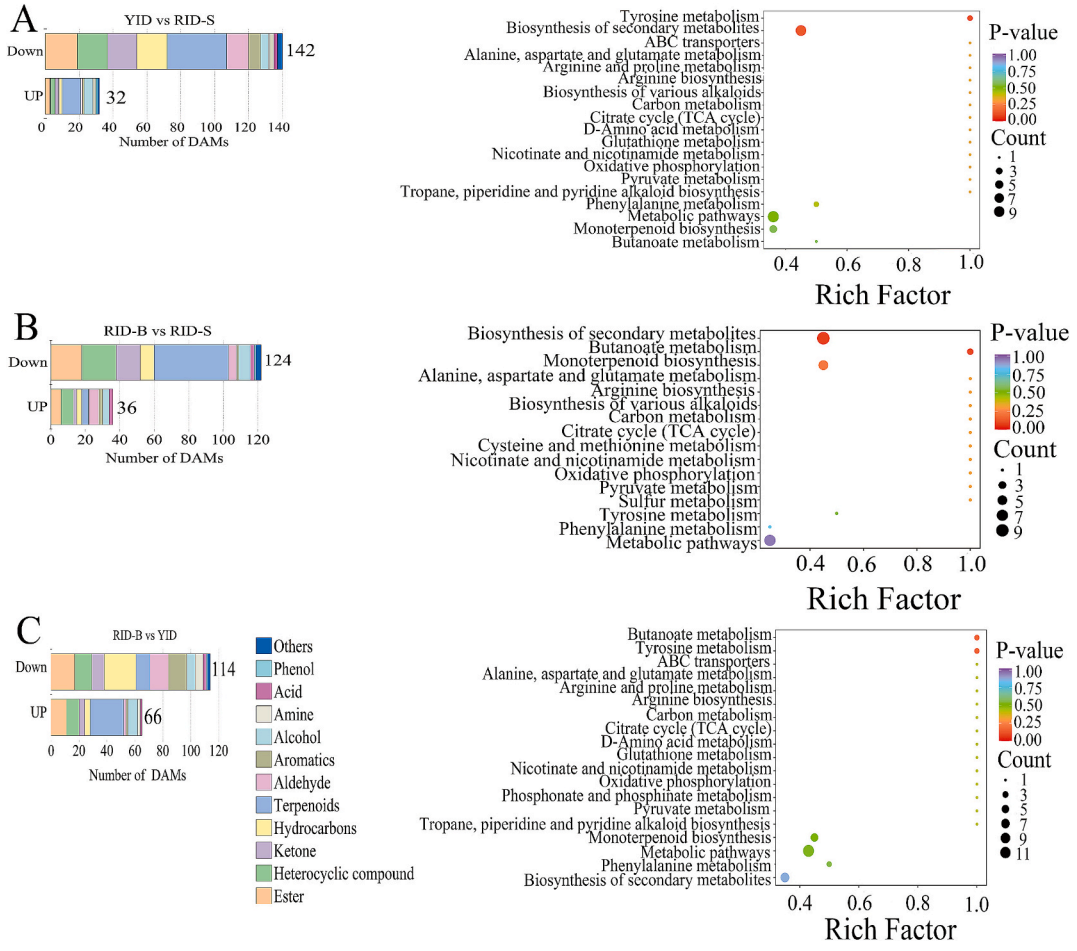

Fig. 4. Distribution of characterized metabolites and their KEGG enrichment analysis in three different phenotypic traits of *IPFO*.

with 10 % deionized water and again centrifuged (3500 r/m) for 30 min to separate the oil samples. Then, the oil samples were bleached and deodorized, and they were distilled under vacuum. Finally, the oil was mixed with a certain amount of deionized water and heated under vacuum with constant stirring for 1 h (95–97 °C). The experiment was repeated three times, and the essential oils were stored in a refrigerator (4 °C) for further analysis.

2.7. Analysis of volatiles

An electronic nose (PEN3, AIRSENSE, China) was employed for the detection of the flavor of the *IPFO* samples from cultivars with varying phenotypic traits. Two grams of each sample was weighed and placed in a centrifuge tube, which was subsequently sealed and allowed to stand for 30 min before testing. The samples were collected at 1 s/group, with an injection flow rate of 400 mL/min and an analysis sampling time of 100 s. The results were collected and analyzed from 68 to 70 s of experimental time. Three replicates were conducted for each sample.

The volatile metabolites in the oil samples were analyzed via HS-SPME (SPME Arrow, CTC Analytics AG, Switzerland) and GC–MS (-7000D, Agilent, China). The samples were prepared using divinylbenzene-carboxene-polydimethylsiloxane fibers with a thickness of 120 μm (DVB-CWR-PDMS), and they were subsequently placed in headspace vials. The samples were then oscillated at 60 °C for 5 min and adsorbed in the headspace for an additional 15 min before desorption at 250 °C for 5 min. The chromatographic conditions were modified according to the methodology proposed by Deng et al. (2024), who utilized a DB-5MS capillary column (30 m × 0.25 mm × 0.25 μm, Agilent J&W Scientific, Folsom, CA, USA) and high-purity helium (≥ 99.999 %) as the carrier gas at a constant flow rate of 1.2 mL/min. The temperature of the GC oven was initially set to 40 °C for 3.5 min, after which it was increased to 100 °C at a rate of 10 °C/min, again increased to 180 °C at a rate of 7 °C/min, and finally increased to 280 °C at a rate of 25 °C/min, which was maintained for 5 min.

2.8. Fatty acid composition analysis

Sample pretreatment: Fifty microliters of thawed sample were added to a centrifuge tube, and 150 μL of the methanol solution, 200 μL of the methyl tert-butyl ether solution, and 50 μL of the 36 % phosphoric acid solution were added to the centrifuge tube. The mixture was vortexed for 3 min and then centrifuged at 4 °C and 12,000 r/min for 5 min. Two hundred microliters of the supernatant were transferred, and the mixture was dried via a nitrogen blower. Three hundred microliters of the 15 % boron trifluoride methanol solution were added, the mixture was vortexed for 3 min, and it was then incubated in an oven at 60 °C for 30 min. After the sample had cooled to room temperature, 500 μL of the n-hexane solution and 200 μL of the saturated sodium chloride solution were added to the centrifuge tube, which was vortexed for 3 min and centrifuged at 4 °C and 12,000 r/min for 2 min, and 100 μL of the upper solution was then transferred for machine analysis. Referring to the chromatographic conditions reported by Kang et al. (2024), a DB-5MS capillary column (30 m × 0.25 mm × 0.25 μm) was employed, with helium serving as the carrier gas. The injection volume was set to 1 μL without splitting, and a constant flow rate of 1 mL/min was maintained. The starting temperature of the heating program was 40 °C (2 min), which was then increased to 200 °C at a rate of 30 °C/min (1 min), increased again to 240 °C at a rate of 10 °C/min (1 min), and finally

Table 3
Differences in the fatty acid composition and content of *IPFO*.

ingredient	Fatty acid content (μg/mL)		
	RID-S	RID-B	YID
decanoic acid	2.00 ± 0.11^{a}	2.24 ± 0.04^{a}	2.00 ± 0.18^{a}
nonanoic acid	2.26 ± 0.17^{a}	2.37 ± 0.30^{a}	2.27 ± 0.35^{a}
myristoleic acid	1.46 ± 0.08^{b}	1.36 ± 0.09^{b}	2.90 ± 0.32^{a}
trans-13-docosenoic acid	3.56 ± 0.24^{b}	4.88 ± 0.30^{a}	3.59 ± 0.33^{b}
octanoic acid	1.86 ± 0.08^{b}	2.32 ± 0.04^{a}	1.98 ± 0.16^{b}
hexanoic acid	0.88 ± 0.04^{b}	0.96 ± 0.01^{a}	0.86 ± 0.05^{b}
lignoceric acid	47.52 ± 1.89^{b}	58.06 ± 1.81^{a}	62.87 ± 5.86^{a}
tricosanoic acid	13.51 ± 0.35^{b}	13.98 ± 0.54^{b}	15.89 ± 1.43^{a}
heneicosanoic acid	0.26 ± 0.01^{a}	0.28 ± 0.01^{a}	0.26 ± 0.01^{a}
lauric acid	9.16 ± 0.61^{b}	12.85 ± 0.35^{a}	8.55 ± 0.87^{b}
tridecanoic acid	0.42 ± 0.01^{b}	0.45 ± 0.01^{ab}	0.47 ± 0.03^{a}
myristic acid	28.70 ± 1.74^{ab}	31.87 ± 0.88^{a}	25.24 ± 2.45^{b}
pentadecanoic acid	3.95 ± 0.22^{c}	5.49 ± 0.13^{b}	11.00 ± 1.07^{a}
palmitic acid	928.12 ± 45.74^{ab}	863.72 ± 19.06^{b}	976.70 ± 66.71^{a}
cis-9-palmitoleic acid	208.70 ± 7.80^{b}	190.91 ± 5.71^{b}	252.00 ± 16.84^{a}
hexadecanedioic acid	1.89 ± 0.05^{a}	1.94 ± 0.03^{a}	1.80 ± 0.03^{b}
heptadecanoic acid	6.70 ± 0.38^{b}	8.67 ± 0.23^{a}	9.27 ± 0.88^{a}
stearic acid	211.11 ± 9.57^{a}	228.43 ± 5.11^{a}	214.54 ± 12.16^{a}
cis-9-octadecenoic acid	505.96 ± 7.67^{c}	547.02 ± 8.21^{b}	604.04 ± 31.90^{a}
linoleic acid	1633.25 ± 61.49^{b}	1807.21 ± 31.72^{a}	1639.25 ± 106.31^{b}
α-linolenic acid	101.10 ± 4.76^{a}	102.17 ± 1.08^{a}	77.33 ± 3.64^{b}
γ-linolenic acid	1.81 ± 0.04^{c}	2.03 ± 0.07^{b}	2.68 ± 0.11^{a}
nonadecylic acid	1.57 ± 0.06^{c}	1.89 ± 0.04^{b}	2.45 ± 0.18^{a}
arachidic acid	23.00 ± 1.24^{b}	26.49 ± 0.79^{b}	30.86 ± 2.75^{a}
cis-11,14-eicosadienoic acid	3.29 ± 0.10^{c}	4.43 ± 0.11^{a}	3.79 ± 0.23^{b}
heneicosanoic acid	3.67 ± 0.20^{c}	4.31 ± 0.10^{b}	5.66 ± 0.43^{a}
behenic acid	37.26 ± 2.18^{b}	37.58 ± 1.03^{b}	55.52 ± 4.83^{a}
erucic acid	7.13 ± 0.62^{a}	5.07 ± 0.26^{b}	5.81 ± 1.29^{ab}
cis-13,16-docosadienoic acid	3.53 ± 0.01^{a}	3.50 ± 0.02^{a}	3.51 ± 0.04^{a}
saturated fatty acid	1334.52 ± 65.53^{a}	1313.84 ± 31.09^{a}	1437.60 ± 102.03^{a}
unsaturated fatty acid	2459.10 ± 81.95^{a}	2658.62 ± 47.01^{a}	2585.50 ± 159.39^{a}

Note: When $p < 0.05$, differences between samples are indicated by "a, b".

increased to 285 °C at a rate of 5 °C/min (3 min).

2.9. Statistical analysis

Each set of experiments was performed three times in parallel, and the data obtained are expressed as the means ± standard deviations. Data processing was conducted via Microsoft Excel 2021. The data were analyzed for significance via SPSS 26.0 software, with $P < 0.05$ indicating significant differences. Plotting was performed via Origin 2024 and TBtools.

3. Results and discussion

3.1. Analysis of phenotypic traits

The color of the pericarp of *I. polycarpa* is determined primarily by the presence of carotenoids and anthocyanins, which impart yellow, orange, and red hues(Hermanns et al., 2020). In particular, anthocyanins are responsible for the production of pink, red, blue, and purple shades (Fan et al., 2023; Rakic & Ulrih, 2021; Zeng et al., 2024). Fig. 1A and B show the variations in the fresh and dry *I. polycarpa* samples, respectively, throughout the drying process. As the collected fruits were subjected to temperature and pressure, decomposition of carotenoids and anthocyanins occurred, resulting in a reduction in yellow and red pigment contents. Additionally, browning and melanin accumulation resulted in fruit blackening. The results revealed no significant difference in fruit color between the fresh samples (Table S1). Conversely, among the dry samples, the YID trait of *I. polycarpa* presented maximum a* and b* values, indicating high contents of carotenoids and anthocyanins. Additionally, the L* values demonstrated a maximum in RID-S, followed by a minimum in RID-B, which is consistent with the findings of Kim et al. (2021).

The characterization of fruit phenotypic traits is crucial for the identification of varieties and the classification of species on the basis of the expression of genetic material(Hermanns et al., 2020; Nankar et al., 2020). Fig. 1 C, D and E show the characteristics of three distinct phenotypic traits of *I. polycarpa* fruits. As indicated in Table 1, there were significant differences ($P < 0.05$) in SW, SL, and SAR, as well as in FTD, FLD, FSiI, and FMSS. SL exhibited the following ranking: RID-B > RID-S > YID. Similarly, SW exhibited the sequence of YID > RID-S > RID-B, whereas the mean SAR value demonstrated the order of RID-B > RID-S > YID. Additionally, FTD, FLD, FSiI, and SFM exhibited the following hierarchy: RID-B > YID > RID-S. These results indicated that RID-B *I. polycarpa* fruits were the greatest compared with the other phenotypic characters. NFPS, PMSS, FMSS, SSM, FShI and FSL did not significantly differ ($P > 0.05$), with NFPS indicating the order of RID-S > YID > RID-B, which suggests that RID-S *I. polycarpa* dominated in terms of the number of fruits. Moreover, the mean FShI values of RID-S, RID-B and YID were 0.98, 0.98 and 1.00, respectively. These findings indicate that the shapes of all three fruit types were nearly spherical and that YID was similar in size to RID-S. In summary, sample *I. polycarpa* fruits were affected by enzymatic and nonenzymatic browning reactions, and all the samples presented decreasing a*, b* and L* values after drying. According to the phenotypic characterization, the RID-B phenotype of *I. polycarpa* presented a breeding advantage.

3.2. Spike and fruit trait correlation analysis

SAR and SL are the core parameters for phenotypic characterization of the fruit spikes of *I. polycarpa*, and Table 2 indicates that there was a highly significant positive correlation between them (with a correlation coefficient of 0.842), whereas there was a highly significant negative correlation between SAR and SW (with a correlation coefficient of 0.874). There were highly significant positive correlations between SSM and FMSS (with a correlation coefficient of 0.986) and between FLD and FTD (with a correlation coefficient of 0.942). The FSiI exhibited highly significant positive correlations with the FTD and FLD (with correlation coefficients of 0.986 and 0.984, respectively). SFM exhibited highly significant positive correlations with FTD, FLD, and FSiI (with correlation coefficients of 0.960, 0.957, and 0.976, respectively) ($P < 0.01$). A notably positive correlation was observed between FMC and FSL, SAR, FTD, FLD, FSiI, and SFM (with correlation coefficients of 0.707, 0.811, 0.813, 0.926, 0.928, and 0.945, respectively) ($P < 0.01$). Notably, the correlation between fruit oil content (FOC) and both cobs and fruits did not reach a significant level. However, FOC was positively correlated with SW and PMSS. In conclusion, the larger the fruit is, the greater the mass of the individual fruit, the longer the stalk of the cob, the larger and heavier the fruit, and the higher the water content of the fruit.

3.3. Water content, oil content and electronic nose analysis

As a wild plant, *I. polycarpa* has been subjected to natural selection and natural hybridization for a long time, resulting in a multitude of variations. Prior studies have revealed significant interpopulation and interindividual differences among *I. polycarpa* species, not only in terms of phenotypic traits such as the pedicel(Wen et al., 2022), flower spike, and fruits but also in terms of the oil and water contents. Therefore, fruit quality is the key to suitable seed selection. The average water contents in the fresh YID, RID-S and RID-B fruits were 34.92 %, 35.04 % and 51.90 %, respectively, and the average oil contents in the dry fruits were 20.63 %, 19.69 % and 17.67 %, respectively (Fig. 2A). The RID-S and

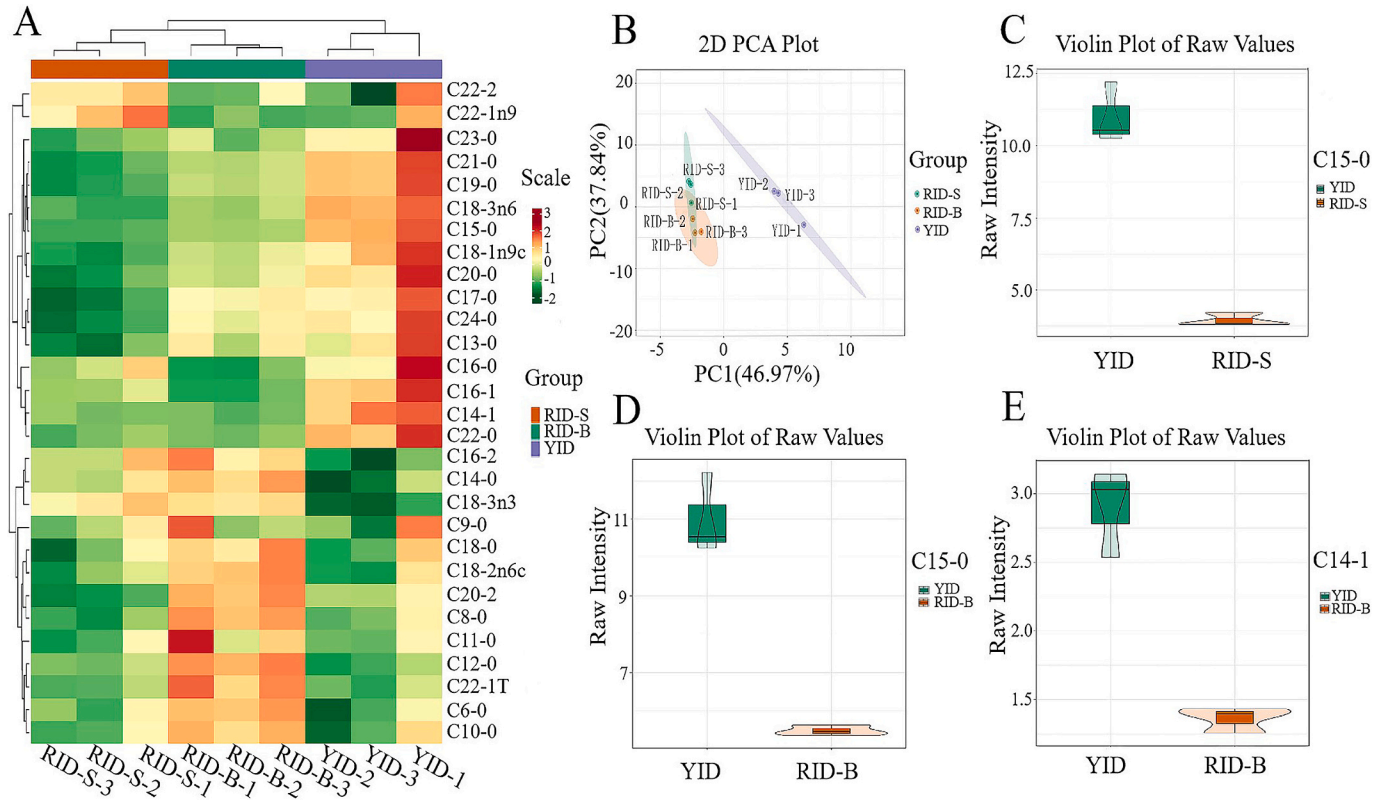

Fig. 5. Fatty acid composition analysis of *I. polycarpa*. (A) Clustering heatmap. The horizontal coordinate represents the sample name, the vertical coordinate denotes the metabolite information, and the varying colors indicate different values obtained from the standardized treatment of varying contents (red represents high content and green represents low content). (B) PCA plot. PC1 represents the first principal component, PC2 represents the second principal component, and the circles represent 95 % confidence intervals. (C, D, E) Differential metabolite violin plots. The box shape in the center represents the interquartile range, the thin black line extending from it represents the 95 % confidence interval, the black horizontal line in the center represents the median, and the outer shape represents the distribution density of the data. (For interpretation of the references to color in this figure legend, the reader is referred to the web version of this article.)

YID samples presented the most similar oil and water content proportions. In contrast, the RID-B sample presented the highest water content and the lowest oil content, which may be attributed to the comparable fruit sizes between the RID-S and YID samples, whereas the RID-B sample was relatively larger in size. Notably, with increasing water content, the oil content decreased, which suggests competition between water and oil in the fruit. However, the relationships between fruit color and water and oil contents must be further verified.

The characteristics of electronic nose detection technology include high sensitivity(Lu et al., 2022), short response times(Feltes et al., 2024), and high detection speeds(Wang & Chen, 2024). This technique was employed to identify and analyze the various types of aroma substances in the *IPFO*. Fig. 2B shows that the contribution rates of Principal Components 1 and 2 were 83.867 % and 13.339 %, respectively, and the cumulative contribution rate exceeded 9 %. However, the spatial distances of the three samples were relatively similar, indicating that the three samples exhibited no significant differences with respect to the first and second principal components. This may be evidence that the samples originated from a single species and thus presented greater aromatic similarity. Therefore, the volatile metabolites were subjected to further examination via GC–MS.

3.4. Volatile component analysis

Volatile organic compounds (VOCs) are integral constituents of fruit nutrients and are essential for fruit aroma, flavor, disease resistance, insect resistance, and finishing quality(Li et al., 2024). TIC plots of mass spectrometry analyses of different phenotypic traits of *I. polycarpa* were shown in Fig. S1. A total of 532 compounds were identified in *IPFO* via a dual detection platform of chromatography and mass spectrometry. The main components included terpenoids (21.62 %), heterocyclic compounds (15.6 %), esters (15.6 %), hydrocarbons (9.77 %), alcohols (8.46 %), ketones (8.08 %) and aldehydes (7.89 %), as shown in Fig. 3A. The volatile compounds were found to be more abundant in the fruits of *I. polycarpa* RID-S, followed by RID-B and YID. The discrepancies observed may be attributed to the presence of specific metabolites associated with particular traits of *I. polycarpa*, while the overall metabolite composition of the three fruit types exhibited a common trend, with lorol, (Z)-3,7-dimethyl-1,3,6-octadecanetriene, (+)-limonene, and benzyl alcohol representing the predominant flavor compounds. Terpenoids were the predominant secondary metabolite among all the samples. This group of substances not only enhances fruit disease resistance but also imparts color, flavor and aroma to the fruit(Huang et al., 2022). The detection of metabolites can facilitate the isolation and identification of *IPFO* functional compounds(Cao et al., 2022).

The samples were subjected to principal component analysis (PCA) to elucidate the differences observed in the *I. polycarpa* fruits. The two principal components (PC1 and PC2) accounted for 38.25 % and 50.46 %, respectively, of the total variance (Fig. 3B). The clustering of all three replicates of each sample in the figure suggests a high degree of reproducibility, indicating data reliability. A significant difference was observed between YID and RID-B on the PC1 axis, which is likely attributable to the red color of RID-B and the distinctive yellow color of YID. On the PC2 axis, YID exhibited significant divergence from RID-S. In terms of morphology, that of YID was greater than that of RID-S, and the accumulated metabolites exhibited notable differences. Compared with PCA, OPLS-DA is more effective in extracting information regarding intergroup differences and in predicting the grouping of

samples. Fig. S 2A, B, and C show notable differences between the three distinct phenotypic traits of *I. polycarpa*. The OPLS-DA model exhibited R^2X values of 0.824, 0.87, and 0.824 for RID-B vs. RID-S, YID vs. RID-B, and YID vs. RID-S, respectively, with an R^2Y value of 1 and a Q^2 value exceeding 0.9. These findings further substantiated the reproducibility and dependability of the experimental outcomes. The thermogram clearly indicated two distinct classes of *I. polycarpa* (Fig. 3E). The correlation coefficients between RID-S and RID-B and between RID-S and YID ranged from 0.76 to 0.78 and from 0.81 to 0.83, respectively. Similarly, the correlation coefficients between RIB and YID ranged from 0.65 to 0.68 (Fig. 3C). The Pearson correlation coefficients of RID-S and YID were the closest to 1, indicating a strong correlation. This finding is consistent with the heatmap results. In conclusion, *I. polycarpa* from the same regional variety did not yield a compact cluster. However, RID-B exhibited distinctive differentiation from RID-S and YID. This suggests that there may be considerable variation in *I. polycarpa.* The other two traits indicated that RID-B could adapt to diverse environmental conditions and possessed a notable capacity for survival.

3.5. Characteristic metabolite analysis

To gain insight into metabolism and to identify differentially abundant metabolites between groups, K-means analysis was employed to identify characteristic metabolites in *IPFO* for different phenotypic traits. A total of 532 metabolites were classified into eight subfamilies (Fig. S3, with each subset showing a similar distribution pattern). The most abundant metabolites in Subfamilies 2, 3, and 8 were RID-S, RID-B, and YID, respectively. These high-abundance subfamilies were identified as characteristic metabolites of the fruits(Zhou et al., 2024). Fig. 3D shows the compositions of these characteristic metabolites. Metabolites characterized from the RID-S vs. RID-B, RID-S vs. YID, and RID-B vs. YID models exhibited a predominant focus on three classes of compounds: terpenoids, heterocyclics, and esters (Fig. S4). Notably, the number of characterized metabolites of YID was considerably smaller than that of RID-S and RID-B, both in terms of quantity and composition. By comparatively analyzing the different metabolites, we obtained a greater understanding of the compositional differences among the three distinct phenotypic traits of *I. polycarpa officinalis*. This analysis also provides a theoretical basis for the development and application of its targeting ability. On the basis of the variable importance in projection (VIP) score and fold change criteria ($\geq$2 or $\leq$ 0.5), 160 differentially accumulated metabolites (DAMs) were identified as significantly different between RID-B and RID-S (36 upregulated and 124 downregulated), 180 DAMs were identified between RID-B and YID (66 upregulated and 114 downregulated), and 174 DAMs were identified between RID-S and YID (32 upregulated and 142 downregulated) (Fig. 4). The metabolites Pyridine, 2-pentyl-, methyl 2-hydroxy-4-methylpentanoate and leucovorin were found to be effective in differentiating between RID-B, RID-S and YID. Among these metabolites, 43 were characterized as commonly shared (Fig. 3F). The Kyoto Encyclopedia of Genes and Genomes (KEGG) database is a powerful tool for analyzing metabolic pathways and metabolic networks(Zou et al., 2020), and it provides annotations for the detected DAMs for pathway enrichment analysis(Zhou et al., 2024). A total of 16 and 19 enriched pathways were identified between RID-B and RID-S and YID, respectively, and 19 were identified between RID-S and YID (Fig. 4). The enrichment of these metabolites was largely concentrated in metabolic pathways (ko01100) and secondary metabolite synthesis (ko01110). In summary, there are large differences in the different phenotypic traits of *I. polycarpa*. Among the same species of *I. polycarpa*, terpenoid, heterocyclic and ester compounds are among the main causes of flavor differences. This suggests that there is rich variation in *I. polycarpa* between species and that there is great potential for breeding between species.

3.6. Fatty acid composition analysis

The composition and value of *IPFO* represent a significant topic for research, given its status as an important woody oil seed crop. Fatty acid composition is a crucial parameter for assessing the quality of *IPFO*. It can effectively reflect its nutritional value and functional properties, thereby guiding individuals to select an appropriate edible oil to achieve a balanced diet (Manolis et al., 2023; Oh et al., 2021; Sharifi et al., 2022). A total of 29 distinct fatty acids were identified in the samples representing the three traits of *IPFO*. Among these fatty acids, 20 were saturated fatty acids, and 9 were unsaturated fatty acids. The top three fatty acids present were LA, palmitic acid, and oleic acid. Among the aforementioned compounds, LA presented the highest concentration in RID-B (1,633.25–1807.21 μg/mL) (Table 3). The predominant fatty acid in *IPFO* was LA, which is of notable nutritional value. An increase in LA intake can result in a moderate reduction in the risk of cancer mortality (Li et al., 2020). The thermogram clearly shows the fatty acid composition of the oil materials (Fig. 5A). The results indicated a notable distinction between palmitic acid and LA in *IPFO*, which can be classified into two distinct groups. Additionally, there was notable variation in the LA content among the oils, which can be grouped into a single category. Notably, RID-B presented a relatively high concentration of LA and a relatively low concentration of palmitic acid. The fatty acid composition was subjected to PCA to evaluate the quality of the *IPFO*. The principal components, PC1 and PC2, accounted for 46.97 % and 37.84 %, respectively, of the total variance, as shown in Fig. 5B. There was no significant difference between RID-B and RID-S. However, there was a significant difference between YID and both RID-B and RID-S, which conforms with the findings of the thermogram. A total of 2 DAMs (myristoleic acid and pentadecanoic acid) were detected in YID vs. RID-B on the basis of a fold change of $\geq$2 or $\leq$ 0.5, and one DAM, i.e., pentadecanoic acid, was detected in YID vs. RID-S. All of these metabolites were significantly upregulated and differed significantly (Fig. 5C, D, and E). Furthermore, the unsaturated fatty acid content in *IPFO* demonstrated notable characteristics. RID-B *IPFO* presented a high concentration of unsaturated fatty acids and a minimal amount of saturated fatty acids, whereas YID *IPFO* presented the highest saturated fatty acid content and the second-highest concentration of unsaturated fatty acids. These findings suggest that RID-B *IPFO* has high nutritional value and that YID *IPFO* is highly stable. In summary, the analysis revealed notable differences between the fatty acid fraction compositions of *IPFO* derived from RID-S and those obtained from RID-B and YID. This suggests that the quality of *IPFO* from RID-S was inferior, with that from YID being of lesser quality, whereas RID-B exhibited the highest quality.

4. Conclusions

The chemical composition of plants may change during growth, which can influence the flavor and oil content of fruits to varying degrees. In this study, we characterized the differences between various phenotypic traits of *I. polycarpa* fruits of the same variety. The data obtained are crucial for understanding the potential nutritional and economic utility of *IPFO*. Under identical cultivation conditions, notable variations exist between fruits of the same variety not only in terms of color and morphological characteristics but also in terms of the oil content, fatty acid composition, and various chemical compositions. The principal aroma compounds in *IPFO* are terpenes, heterocyclic compounds, and esters. The main polyunsaturated fatty acids in the fruit are LA, oleic acid, and palmitic acid. The highest concentration of LA was detected in RID-B fruit oil, which has excellent *I. polycarpa* cultivation value. These findings offer insights into the enhancement of *I. polycarpa* fruit quality and the development of functional foods. Additionally, this study provides a valuable reference for the selection and breeding of *I. polycarpa* varieties.

CRediT authorship contribution statement

Tianting Luo: Writing – original draft, Methodology, Formal analysis, Conceptualization. **Jiaqi Xu:** Validation, Methodology, Investigation, Data curation. **Zhouqin Zhen:** Validation, Investigation. **Xue Pan:** Software, Data curation. **Lang Feng:** Software. **Likang Qin:** Supervision, Data curation. **Tingyuan Ren:** Writing – review & editing, Visualization, Supervision, Resources, Project administration, Funding acquisition.

Declaration of competing interest

The authors declare that they have no known competing financial interests or personal relationships that could have appeared to influence the work reported in this paper.

Data availability

Data will be made available on request.

Acknowledgments

This work was supported by the Guizhou Provincial Science and Technology Major Special Project (Qiankehe Major Special Project [2024] No. 025).

Appendix A. Supplementary data

Supplementary data to this article can be found online at https://doi.org/10.1016/j.fochx.2024.102127.

References

Bowen, R. A., & Clandinin, M. T. (2005). Maternal dietary 22 : 6n-3 is more effective than 18 : 3n-3 in increasing the 22 : 6n-3 content in phospholipids of glial cells from neonatal rat brain. *British Journal of Nutrition, 93*(5), 601–611. https://doi.org/10.1079/bjn20041390

Cao, Y., Ren, M., Yang, J., Guo, L., Lin, Y., Wu, H., … Wang, H. (2022). Comparative metabolomics analysis of pericarp from four varieties of Zanthoxylum bungeanum maxim. *Bioengineered, 13*(6), 14815–14826. https://doi.org/10.1080/21655979.2022.2108632

Chakraborty, K., & Joseph, D. (2015). Production and characterization of refined oils obtained from Indian oil sardine (*Sardinella longiceps*). *Journal of Agricultural and Food Chemistry, 63*(3), 998–1009. https://doi.org/10.1021/jf505127e

Deng, J., Zhao, H., Qi, B., Wang, D., Wu, Y., Dai, S., Xia, J., Lu, M., Yao, K., Ma, A., & Jia, Y. (2024). Volatile characterization of crude and refined walnut oils from aqueous enzymatic extraction by GC-IMS and GC-MS. *Arabian Journal of Chemistry, 17*(1). https://doi.org/10.1016/j.arabjc.2023.105404

Dyer, J. M., Stymne, S., Green, A. G., & Carlsson, A. S. (2008). High-value oils from plants. *The Plant Journal, 54*(4), 640–655. https://doi.org/10.1111/j.1365-313x.2008.03430.x

Eguchi, K., Manabe, I., Oishi-Tanaka, Y., Ohsugi, M., Kono, N., Ogata, F., Yagi, N., Ohto, U., Kimoto, M., Miyake, K., Tobe, K., Arai, H., Kadowaki, T., & Nagai, R. (2012). Saturated fatty acid and TLR signaling link β cell dysfunction and islet inflammation. *Cell Metabolism, 15*(4), 518–533. https://doi.org/10.1016/j.cmet.2012.01.023

Fan, M., Li, X., Zhang, Y., Yang, M., Wu, S., Yin, H., Liu, W., Fan, Z., & Li, J. (2023). Novel insight into anthocyanin metabolism and molecular characterization of its key regulators in *Camellia sasanqua*. *Plant Molecular Biology, 111*(3), 249–262. https://doi.org/10.1007/s11103-022-01324-2

Feltes, G., Ballen, S. C., Soares, A. C., Soares, J. C., Paroul, N., Steffens, J., & Steffens, C. (2024). Discrimination of artificial strawberry aroma by electronic nose based on nanocomposites. *Journal of Food Process Engineering, 47*(1). https://doi.org/10.1111/jfpe.14501

Hermanns, A. S., Zhou, X., Xu, Q., Tadmor, Y., & Li, L. (2020). Carotenoid pigment accumulation in horticultural plants. *Horticultural Plant Journal, 6*(6), 343–360. https://doi.org/10.1016/j.hpj.2020.10.002

Huang, Y., Xie, F., Cao, X., & Li, M. (2022). Research progress in biosynthesis and regulation of plant terpenoids. *Biotechnology & Biotechnological Equipment, 35*(1), 1799–1808. https://doi.org/10.1080/13102818.2021.2020162

Kang, J., Yue, Y., Wei, S., Chen, H., & Luo, P. (2024). Superior component compositions and antioxidant activity of Volvariella volvacea oil compared to those of Agrocybe cylindracea and two Lentinula edodes oils. *Food Science & Nutrition, 12*(1), 268–279. https://doi.org/10.1002/fsn3.3750

Kim, S., Kim, S., Shim, I., Hong, E., & Kim, S. (2021). Drying operation effects on the pigments and phytochemical properties of rose cultivars. *Journal of AOAC International, 104*(4), 1148–1154. https://doi.org/10.1093/jaoacint/qsab064

Li, B., Ren, T., Yang, M., Lu, G., & Tan, S. (2024). Assessment of quality differences between wild and cultivated fruits of *Rosa roxburghii* Tratt. *LWT- Food Science and Technology, 202*, Article 116300. https://doi.org/10.1016/j.lwt.2024.116300

Li, J., Guasch-Ferré, M., Li, Y., & Hu, F. B. (2020). Dietary intake and biomarkers of linoleic acid and mortality: Systematic review and meta-analysis of prospective cohort studies. *American Journal of Clinical Nutrition, 112*(1), 150–167. https://doi.org/10.1093/ajcn/nqz349

Liu, R., He, X., Wen, L., Guo, Z., Zhu, Q., Wei, M., … Liu, R. (2023). Differences in chemical composition and fatty acid composition of fruits from different provenances and families of Idesia polycarpa. *Acta Agriculturae Universitatis Jiangxiensis, 45*(05), 1072–1083. https://doi.org/10.13836/j.jjau.2023099

Lu, L., Hu, Z., Hu, X., Li, D., & Tian, S. (2022). Electronic tongue and electronic nose for food quality and safety. *Food Research International, 162*, Article 112214. https://doi.org/10.1016/j.foodres.2022.112214

Lummiss, J. A. M., Oliveira, K. C., Pranckevicius, A. M. T., Santos, A. G., Dos Santos, E. N., & Fogg, D. E. (2012). Chemical plants: High-value molecules from essential oils. *Journal of the American Chemical Society, 134*(46), 18889–18891. https://doi.org/10.1021/ja310054d

Manolis, A. A., Manolis, T. A., Melita, H., & Manolis, A. S. (2023). Features of a balanced healthy diet with cardiovascular and other benefits. *Current Vascular Pharmacology, 21*(3), 163–184. https://doi.org/10.2174/1570161121666230327135916

Marangoni, F., Agostoni, C., Borghi, C., Catapano, A. L., Cena, H., Ghiselli, A., … Poli, A. (2020). Dietary linoleic acid and human health: Focus on cardiovascular and cardiometabolic effects. *Atherosclerosis, 292*, 90–98. https://doi.org/10.1016/j.atherosclerosis.2019.11.018

Mena, C., Gonzalez, A. Z., Olivero-David, R., & Angeles Perez-Jimenez, M. (2018). Characterization of "Castellana" virgin olive oils with regard to olive ripening. *Horttechnology, 28*(1), 48–57. https://doi.org/10.21273/HORTTECH03845-17

Nankar, A. N., Tringovska, I., Grozeva, S., Ganeva, D., & Kostova, D. (2020). Tomato phenotypic diversity determined by combined approaches of conventional and high-throughput tomato analyzer phenotyping. *Plants-Basel, 9*(2), 197. https://doi.org/10.3390/plants9020197

Oh, Y. J., Nam, K., Kim, Y., Lee, S. Y., Kim, H. S., Kang, J. I., … Hwang, K. T. (2021). Effect of a nutritionally balanced diet comprising whole grains and vegetables alone or in combination with probiotic supplementation on the gut microbiota. *Preventive Nutrition and Food Science, 26*(2), 121–131. https://doi.org/10.3746/pnf.2021.26.2.121

Rakic, V., & Ulrih, N. P. (2021). Influence of pH on color variation and stability of cyanidin and cyanidin 3-*O*-*β*-glucopyranoside in aqueous solution. *CyTA Journal of Food, 19*(1), 174–182. https://doi.org/10.1080/19476337.2021.1874539

Shang, Z., Xu, T., Zou, K., & Ma, L. (2024). Effect of drying method of Idesia polycarpa fresh fruit on the quality of Idesia polycarpa oil. *China Oils and Fats, 49*(01), 11–15. https://doi.org/10.19902/j.cnki.zgyz.1003-7969.220593

Sharifi, M. H., Izadpanah, P., Hosseini, M. M., & Vojoudi, M. (2022). Relationship between dietary variety, adequacy, moderation, and balanced diet and cardiovascular risk factors. *BMC Nutrition, 8*(1), 20. https://doi.org/10.1186/s40795-022-00514-x

Shi, T., Wu, G., Jin, Q., & Wang, X. (2020). Camellia oil authentication: A comparative analysis and recent analytical techniques developed for its assessment. A review. *Trends in Food Science & Technology, 97*, 88–99. https://doi.org/10.1016/j.tifs.2020.01.005

Šimat, V., Vlahović, J., Soldo, B., Skroza, D., Ljubenkov, I., & Generalić, M. I. (2019). Production and refinement of Omega-3 rich oils from processing by-products of farmed fish species. *Foods, 8*(4), 125. https://doi.org/10.3390/foods8040125

Wang, M., & Chen, Y. (2024). Electronic nose and its application in the food industry: A review. *European Food Research and Technology, 250*(1), 21–67. https://doi.org/10.1007/s00217-023-04381-z

Wen, L., Xiang, X., Wang, Z., Yang, Q., Guo, Z., Huang, P., Mao, J., An, X., & Kan, J. (2022). Evaluation of cultivars diversity and lipid composition properties of Idesia polycarpa var. vestita Diels. *Journal of Food Science, 87*(9), 3841–3855. https://doi.org/10.1111/1750-3841.16293

Wu, T., Duan, Z., & Wang, C. (2023). Effects of microwave drying on color change, phenolic substance content and phenolase activity of different parts of persimmon slices. *Journal of Food Measurement and Characterization, 18*, 357–369. https://doi.org/10.1007/s11694-023-02162-6

Zeng, H., Zheng, T., Tang, Q., Xu, H., & Chen, M. (2024). Integrative metabolome and transcriptome analyses reveal the coloration mechanism in *Camellia oleifera* petals with different color. *BMC Plant Biology, 24*(1), 19. https://doi.org/10.1186/s12870-023-04699-6

Zhao, M., Xu, J., Liu, Y., Li, P., Liu, Z., Li, Z., … Wang, Y. (2024). Analysis of fruit of Idesia polycarpa maxim at different harvest periods. *Journal of Henan Agricultural University, 58*(01), 69–77. https://doi.org/10.16445/j.cnki.1000-2340.20231213.001

Zhou, M., Sun, Y., Mao, Q., Luo, L., Pan, H., Zhang, Q., & Yu, C. (2024). Comparative metabolomics profiling reveals the unique bioactive compounds and astringent taste formation of rosehips. *Food Chemistry, 425*, Article 139584. https://doi.org/10.1016/j.foodchem.2024.139584

Zou, S., Wu, J., Shahid, M. Q., He, Y., Lin, S., Liu, Z., & Yang, X. (2020). Identification of key taste components in loquat using widely targeted metabolomics. *Food Chemistry, 323*, Article 126822. https://doi.org/10.1016/j.foodchem.2020.126822

Zuo, Y., Liu, H., Li, B., Zhao, H., Li, X., Chen, J., Wang, L., Zheng, Q., He, Y., Zhang, J., Wang, M., Liang, C., & Wang, L. (2024). The Idesia polycarpa genome provides

insights into its evolution and oil biosynthesis. *Cell Reports, 43*(3). https://doi.org/10.1016/j.celrep.2024.113909